

Comparison of Measurement Strategies for Light Absorbing Aerosols from Modern Diesel Engines

Author, co-author (Do NOT enter this information. It will be pulled from participant tab in MyTechZone)

Affiliation (Do NOT enter this information. It will be pulled from participant tab in MyTechZone)

Copyright © 2014 SAE International

Abstract

Light absorbing components of aerosols, often called black carbon (BC), are emitted from combustion sources and are believed to play a considerable role in direct atmospheric radiative forcing by a number of climate scientists. In addition, it has been shown that BC is associated with adverse health effects in a number of epidemiological studies. Although the optical properties (both absorbing and scattering) of combustion aerosols are needed in order to accurately assess the impact of emissions on radiative forcing, many models use radiative properties of diesel particulate matter that were determined over two decades ago. In response to concerns of the human health impacts of particulate matter (PM), regulatory bodies around the world have significantly tightened PM emission limits for diesel engines. These requirements have resulted in considerable changes in engine technology requiring updated BC measurements from modern engines equipped with aftertreatment systems. In this study, a variety of common ambient monitoring techniques were used to characterize the light absorbing properties of diesel aerosol. Aerosol optical properties were directly measured with an Aethalometer and Photoacoustic Extinctionmeter and compared to filter based analysis. The results showed excellent correlation ($R^2 = 0.95$) between aerosol light absorption at the short IR wavelength with elemental carbon (EC) concentration from a thermal optical reflectance, NIOSH 5040 method. Resulting EC mass absorption cross-section efficiencies differed by 25 to 30% from manufacturer published values indicating the optical properties used by the instrument may not be representative of modern diesel engine emissions.

Introduction

Vehicular emissions are a prominent source of particles found in urban environments [1]. Particulate matter (PM), although remains the only regulated criteria pollutant that is not chemically defined, is one of the most important due to its adverse impact on human health, atmospheric conditions, and climate. A multitude of epidemiological studies have shown an association between ambient PM and harmful cardiovascular and pulmonary health effects [2, 3]. In addition to the health concerns related to PM, the optical behavior of a given aerosol is of growing concern due to its effect on atmospheric radiative forcing [4]. In response to these concerns, worldwide

regulatory bodies have significantly tightened particulate emission limits for light and heavy duty vehicles. Since 2007 in the US, on-highway diesel engines have been using diesel particulate filters (DPFs) to meet PM mass emission standards. However, many off-highway applications are able to meet PM mass emissions standards without a DPF, only using a diesel oxidation catalyst (DOC) and selective reduction catalyst (SCR). The application of modern PM control strategies significantly changes the chemical, physical and optical properties of diesel PM [5]. These changes to the makeup of emitted diesel PM require updated measurement methods to understand the possible environmental impact of control strategies.

Atmospheric modeling has shown that PM mitigation strategies have the potential of reducing mean projected global warming by $\sim 0.5^\circ\text{C}$ by 2050 [6]. Carbonaceous PM can be divided into Black Carbon (BC) and Organic Carbon (OC), where BC has been defined by the U.S. Environmental Protection Agency (EPA) as "a solid form of mostly pure carbon that absorbs solar radiation (light) at all wavelengths." [7]. BC is not the only constituent of PM which affects the radiative forcing potential of an aerosol. A coating of OC has been shown to enhance light absorption at all wavelengths; this phenomena can be explained by the OC behaving like a lens, focusing the incident radiation into the BC core [4]. The term "Brown Carbon" (BrC) has been applied to the absorption of light by OC and is thought to be significant in overall aerosol light absorption measurements. This study aimed to reduce the impact of BrC on absorption measurements, as BrC measurements are still under development and add considerable uncertainty to light absorption.

Controlling BC emission has the near term benefit of reduced global mean radiative forcing as compared to other Green House Gases (GHGs) due to their reduced residence time in the atmosphere. Atmospheric BC concentrations have been measured across the country and the world for over 20 years. In the US, over half of BC emissions in 2005 were due to mobile sources, in which nearly 90% were attributed to diesel engines [7]. Measurements in California have shown the effect of reduction of diesel PM emissions on atmospheric BC concentrations [8]. The determination of optical properties of the aerosol is crucial for the accuracy of radiative transfer modeling, unfortunately many models use values over two

decades old [4]. One of the aims of this work is to compare modern diesel engine BC to historical diesel BC.

Due to increasingly stringent air quality regulations, a large amount of measurement techniques have been developed to quantify aerosol light absorption. These methods have been summarized extensively by Moosmüller [9]. Some of the methods of interest, when regarding diesel engine source testing, include thermal optical reflectance (or transmittance) analysis of quartz particulate matter filters (Elemental Carbon/Organic Carbon), in situ photoacoustic light absorption, and real time quartz filter tape transmission (Aethalometer). Integrated filter based methods are widely accepted but lack time resolution required for transient diesel emissions and have long turnaround time compared to real time instruments [9]. Real time instruments have been developed to correlate with integrated filter measurements (most often EC) [10]. Extensive work has been done characterizing and describing all aforementioned methods and is out of scope of this paper.

The use of aerosol light absorption measurements in a heavy duty diesel emissions lab has been limited. Many resources have been devoted to measuring aged light absorption of atmospheric aerosols [4, 11, 12, 13, 14]. One of the first attempts of light absorption measurement of freshly emitted diesel aerosol from a Constant Volume Sampling (CVS) emissions measurement system was done by Moosmüller et al in 2001. Researchers struggled to measure BC emissions with the aethalometer due to dilution system constraints [15]. Kittelson et al. provided a comparison of carbon measurements using an aethalometer, NIOSH Method 5040 EC/OC integrated filters and a Scanning Mobility Particle Sizer [16]. The authors state, 'Since the aethalometer software uses a constant extinction cross-section value ($16.6 \text{ m}^2 \text{ g}^{-1}$) to calculate BC mass concentration, the importance of field calibration to determine a unique sigma value for various aerosols should be stressed.' [16]. Over the course of this literature review this sentiment of highly uncertain aerosol absorption cross-section efficiency (or sigma) for freshly emitted diesel particulate was common. An analytical solution for the mass specific absorption efficiency gives a framework for understanding BC measurement sensitivity.

Absorption efficiency is a function of particle size (D_p), the wavelength of the incident light (λ) and the complex refractive index of the particle (m). Eq. (1) describes the mass specific absorption efficiency of a smooth homogeneous particle.

$$E_{abs}(D_p, \lambda, m) = \frac{3}{2\rho_p D_p} Q_{abs}(m, \alpha) \quad (1)$$

Where ρ_p is the particle density, Q_{abs} is the dimensionless absorption efficiency and α is the dimensionless size

parameter. Liu et al. offer a comparison of three size resolved particle density corrections [17]. An optical model was run with constant particle density, but varied over the expected range (0.2 g/cc to 1.2 g/cc) to demonstrate the sensitivity of optical properties as a function of particle composition. A numerical solution for Q_{abs} was provided by Bohren and Huffman [18, 19, 20]. Using a MATLAB based Mie theory model, the mass specific absorption efficiency were calculated using a refractive index of $1.68 + 0.56i$ from Bond and Bergstrom [4]. The results are presented in Figure 1.

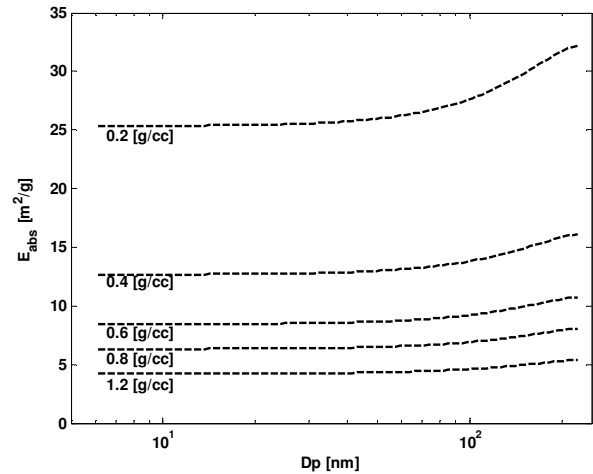


Figure 1: Mass specific particle absorption efficiency for diesel soot

Figure 1 shows that mass specific absorption efficiency at small particle sizes ($< 50 \text{ nm}$) with a constant particle density does not change strongly with particle size. However above 50 nm , mass specific absorption efficiency for a constant particle density can increase by 15% or greater. At a constant particle diameter, the range of expected particle densities can change mass specific absorption efficiency by a factor of 5. This necessitates particle size and composition information for fundamental understanding of diesel PM absorption measurements.

Modern diesel engine emission control strategies are known to change PM composition and particle size distribution (PSD) [5]. Post DPF optical measurements will likely lead to similar conclusions of PM mass reduction (greater than 99% filtration efficiency). However, a large fraction of diesel engines that operate off-highway, are able to meet Tier IV Final regulations without a DPF. This raises the concern of high BC emission rates for engines only equipped with a DOC.

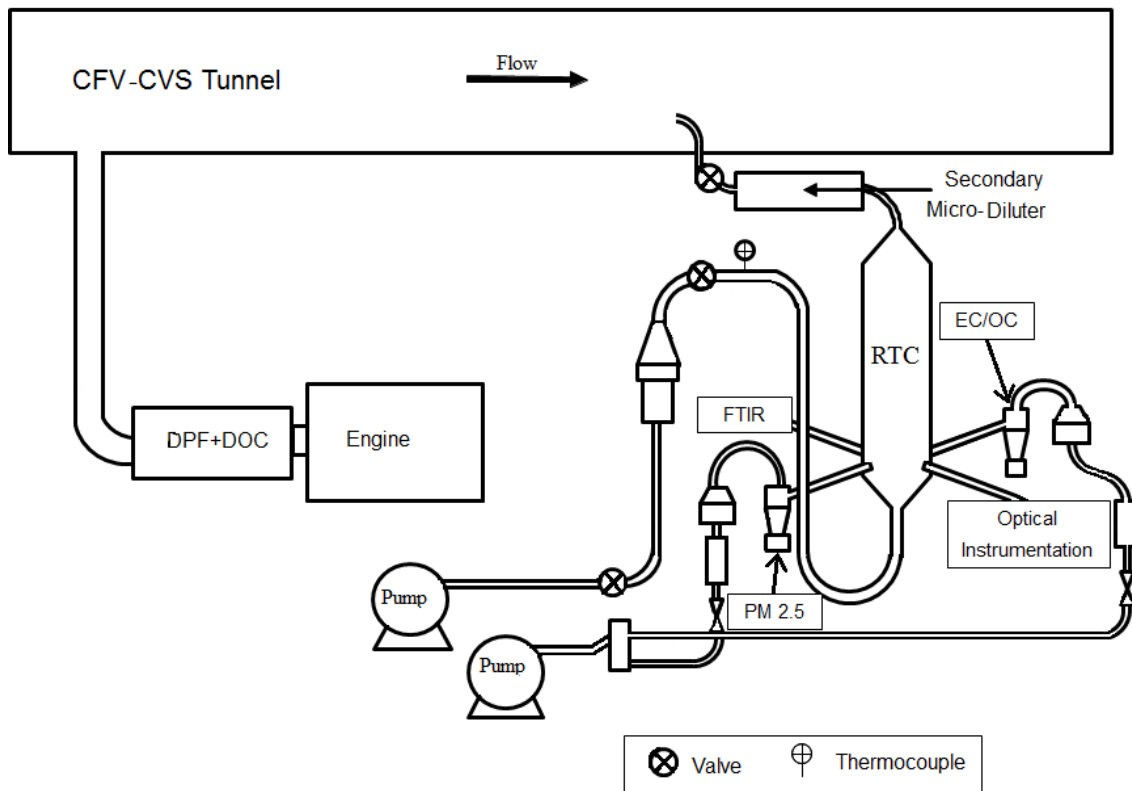


Figure 2: Test Cell and Dilution System Schematic

The goal of the present study was to perform a comparison of the two available direct optical measurements in parallel with filter based methods. In order to gain a more fundamental understanding of factors affecting aerosol optical properties, particle size measurements were also done.

Experimental Methods

Engine Setup

A turbocharged inline 6 cylinder heavy duty diesel engine was tested in this study. This engine uses high pressure common rail direct fuel injection, high pressure exhaust gas recirculation (EGR) and other common combustion strategies used to meet EPA 2010 emissions regulations. A DOC was used to reduce Carbon Monoxide (CO), Total Hydrocarbons (THCs) and some of the soluble organic fraction (SOF) of PM. It must be noted that during this study no selective catalytic reduction (SCR) system was used to reduce nitrogen oxides (NOx), as the effect of SCR on PM optical properties was deemed out of scope. A General Electric 700 HP transient DC dynamometer was used to load the engine over three engine modes described in Table 1. Ultra low sulfur #2 diesel fuel was used during this study. Fuel specifications can be found in Table 2.

Table 1. Engine Operating Conditions

	Idle	B50	C100
Speed	650 RPM	1555 RPM	1912 RPM
Load	10 %	50 %	100 %
Exhaust Temp.	128 °C	341 °C	424 °C

Hot steady state engine operating points were chosen to provide distinct emission composition and particle size distribution over a representative operating map. Hot steady state testing was done to reduce variability in aerosol formation. The engine was warmed up and allowed to stabilize for 30 minutes before any emission samples were taken.

Table 2. Fuel Specifications

Density, 15 °C	845.0 kg/m ³
API Gravity, 16/16 °C	36.0
Viscosity @ 40 °C	2.67 mm ² /s
Flash Point	70 °C
Cetane Number	47.4
Sulfur	6 ppm
Gross Heating Value	45608 kJ/kg
Aromatics	26.3 wt%
Monoaromatics	23.8 wt%
PNA's	2.5 wt%
Distillation Temp.	
	IBP 178.6 °C
	T10 213.6 °C
	T50 260.0 °C
	T90 322.9 °C
	EPT 352.2 °C

Dilution System

In this study an improved source dilution sampling system (SDS) was used in conjunction with a critical flow venturi-constant volume system (CFV-CVS) tunnel to dilute diesel exhaust in a controlled manner [21]. A layout of the dilution system and test cell is presented in Figure 2. The SDS was designed to minimize thermophoretic and electrostatic forces to reduce particle loss. SDS residence time was optimized to allow sufficient time for volatiles and semi-volatile to nucleate, condense and coagulate.

Full engine exhaust flow was piped into the CFV-CVS tunnel, where it is well mixed with HEPA filtered and conditioned dilution air. During the course of the study primary dilution ratio was chosen to meet EPA Part 1065 dilution requirements. HEPA filtered and conditioned secondary dilution air was well mixed with dilute exhaust sampled from the CVS tunnel using an annular type mixing chamber on the SDS. Secondary dilution air was controlled with mass flow controller during the sample period. Secondary dilution ratio was varied during the testing campaign depending on engine mode. The secondary dilution ratio was optimized for filter based and real time optical analytics. Total dilution varied from 30:1 to 50:1.

Direct Measurements

Aethalometer

The aethalometer is an instrument which measures the attenuation of a specific wavelength of light through a quartz fiber filter tape as it loads with aerosol over time. The Magee Scientific Model AE31 aethalometer was used in this study. The AE31 measures attenuation at seven wavelengths, from 370 nm (UV) to 950 nm (IR) in quasi real time (two minute resolution). Light attenuation through the filter tape is defined in Eq. (2).

$$ATN = \ln\left(\frac{I_0}{I}\right) \quad (2)$$

Where I_0 is the intensity of light passing through a “fresh” portion of the filter tape and I is the intensity passing through a loaded filter. As particles deposit on the filter tape during a time period, Δt , ATN at a given λ will increase, such that the n th measurement yields the aerosol attenuation coefficient ($b_{ATN,n}$) shown in Eq. (3).

$$b_{ATN,n}(\lambda) = \frac{(ATN_n(\lambda) - ATN_{n-1}(\lambda)) \cdot A}{\Delta t \cdot V} \quad (3)$$

Where A is the area of the sampling spot and V is the volumetric sample flowrate [22]. Finally to report BC mass concentration, the internal AE31 software uses the mathematical relationship in Eq. (4).

$$M_{BC} = \frac{b_{ATN,n}(\lambda)}{\sigma_{ATN}(\lambda)} \quad (4)$$

Where σ_{ATN} at 880 nm for the AE31 is set to $16.6 \text{ m}^2\text{g}^{-1}$.

Maximum filter attenuation is eventually reached dependent on aerosol concentration and sample flowrate, requiring the filter

tape to advance. This requires careful adjustment of total dilution to prevent filter tape advancement during sampling.

Photoacoustic Extinctionmeter

Photoacoustic aerosol measurements have been shown to be useful for engine development, as the real time in-situ method allows for immediate feedback for combustion recipe and aftertreatment development. The Droplet Measurement Technologies Photoacoustic Extinctionmeter (PAX) was used for this study. The DMT PAX features an 870 nm wavelength modulated diode laser which allows for simultaneous aerosol light scattering and absorption. It should be noted that two minute averages were done on the real time absorption data due to high amounts of noise in the instantaneous signal. The layout of the acoustic chamber is shown in Figure 3.

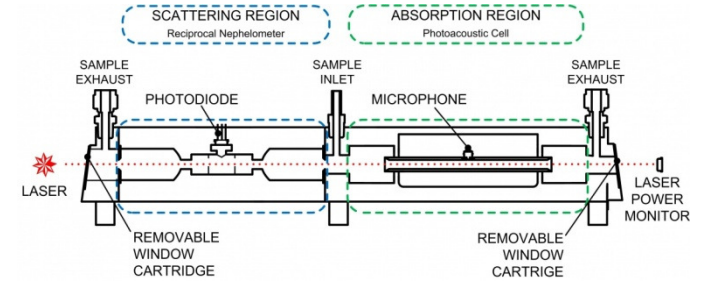


Figure 3: Schematic of DMT PAX Acoustic chamber [23]

The laser beam is directed through the sampled aerosol stream and modulated at the resonance frequency (f_{res}) of the acoustic chamber. Strongly absorbing particles heat up quickly and transfer heat to the surrounding air producing pressure waves that can be detected with a sensitive microphone. Eq. (5) describes the relationship of aerosol absorption coefficient (b_{abs}).

$$B_{abs} = \frac{P_{mic} A_{res} \pi^2 f_{res}}{P_L (\gamma - 1) Q} \cdot \cos \phi \quad (5)$$

Where P_{mic} is the microphone pressure at the given f_{res} for the acoustic chambers conditions (temperature, pressure and relative humidity). A_{res} is the cross sectional area of the resonator, P_L is the laser power, γ is the ratio of isobaric and isochoric specific heat, Q is the resonator quality factor and ϕ is the phase of the B_{abs} signal relative to the laser power phase [23]. Similarly to the AE31, the internal software of the PAX adjusts the absorption coefficient to a mass of BC (Eq. (6)) with a constant mass specific absorption cross-section efficiency (σ_{abs}).

$$M_{BC} = \frac{B_{abs}}{\sigma_{abs}} \quad (6)$$

The PAX software uses a σ_{abs} of $4.74 \text{ m}^2\text{g}^{-1}$. This value came from the Bond and Bergstrom review where fresh soot demonstrated a σ_{abs} of $7.5 \pm 1.2 \text{ m}^2\text{g}^{-1}$ at 550 nm [4]. As σ_{abs} varies inversely with incident wavelength, Eq. (7) describes the σ_{abs} at 870 nm [23].

$$\sigma_{abs}(870) = 7.5 \left[\frac{\text{m}^2}{\text{g}} \right] \cdot \left(\frac{550 \text{ nm}}{870 \text{ nm}} \right) = 4.74 \left[\frac{\text{m}^2}{\text{g}} \right] \quad (7)$$

Particle Size Distribution

Particle size distributions (PSD) were measured with a TSI model 3080 Scanning Mobility Particle Sizer (SMPS). The SMPS, described in detail by Liu et al [24], classifies particles based on differential electrical mobility, via a differential mobility analyzer (DMA) and counts them via a ultrafine condensation nuclei particle counter (TSI model 3025a). The SMPS was configured to measure PSD over a size range of 6.2 – 225 nm across 64 channels per decade with an up-scan time of 120 s. The SMPS was calibrated prior to sampling for flows and voltages. Particle mobility was validated by using polystyrene latex calibration aerosol.

Filter Based Measurements

Two types of PM sampling train setups were used in this study and are shown in Figure 2. Each train begins with a PTFE-coated aluminum PM_{2.5} cyclonic separator. PM was sampled on pre-baked quartz fiber filters (QFF) or TX40 teflon impregnated quartz filters at a nominal flowrate of 16.7 slpm. Flow through each sample train was controlled by downstream critical flow orifices, which were calibrated daily during the study.

Elemental and Organic Carbon Analysis

QFF were analyzed for the elemental and organic carbon (EC/OC respectively) content of the sampled PM via thermal-optical method (NIOSH 5040) using a Sunset Laboratory Lab EC/OC Aerosol Analyzer. EC analytical uncertainty (δEC) is estimated with Eq. (8) [25].

$$\delta EC = 0.05 \left[\frac{\mu g}{cm^2} \right] + 0.05 * EC + 0.05 * PC \quad (8)$$

Where EC is total Elemental Carbon and PC is the pyrolyzed carbon adjustment reported by the analysis.

PM_{2.5} Mass

TX40 filters were analyzed gravimetrically with an EPA Part 1065 compliant MTL filter weighing system. After sampling, filters conditioned for a minimum of 24 hours in the chamber. A Mettler Toledo XPU 2000 microbalance was used for pre and post weighing. Part 1065 buoyancy corrections were applied to all samples.

Results and Discussion

A representative example of the Source Dilution System BC concentration, calculated using the instrument standard mass absorption cross-section efficiencies by the AE31 and PAX are shown in Figure 4. On the secondary axis the SDS particle concentration shows stable particle concentration over the sample period.

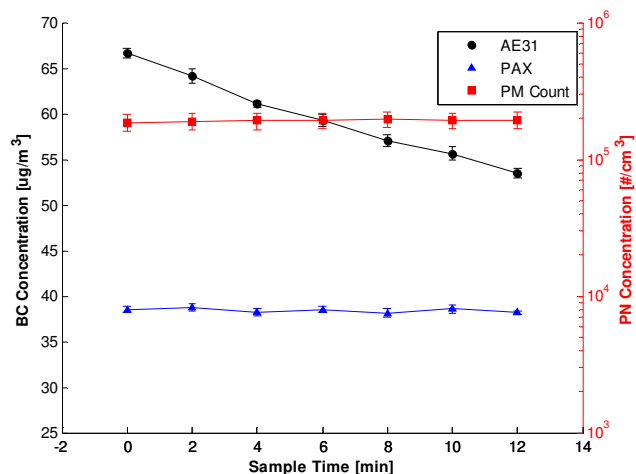


Figure 4: SDS BC and PM number concentration observed during a typical sample period

AE31 BC concentration decreases over the sample period, contrary to the constant particle number and PAX BC concentration. This apparent decrease in BC concentration and filter artifact correction is a complex and heavily studied topic. Aspects of this behavior can be attributed to attenuation enhancements due to multiple scattering by the filter fibers, scattering of aerosols sampled on the filter and the reduction of the optical path as particles accumulate on the filter. These three phenomena are well documented in filter based absorption measurement correction literature [4, 9, 22]. An artifact correction was not applied for this initial measurement comparison study and should be noted when interpreting AE31 data.

Particle size distributions (PSD) are shown for all three engine modes in Figure 5. Error bars represent standard error from 3 separate tests. Significant difference in the Idle PSD from both B50 and C100 PSDs indicates a possible difference in the specific cross-section efficiencies (σ) as a function of engine operation. However when considering the mass specific absorption efficiency curve in Figure 1, it is clear that PSD differences are not significant enough in the given size range to play a major role in BC emissions quantification from modern diesel engines using optical methods. Due to the similar PSDs for each engine operation mode, all engine modes were grouped into a common dataset for determination of specific cross-section efficiencies.

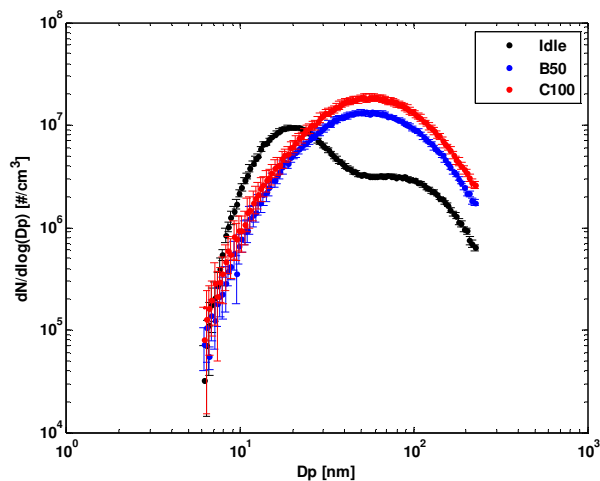


Figure 5: Particle Size Distributions for each engine mode

The AE31 attenuation coefficient (b_{ATN}) at 880 nm was fit against EC concentrations determined by the NIOSH 5040 method. Similarly the PAX absorption coefficient (b_{abs}) at 870 nm was fit against elemental carbon concentrations. The slope of these fits result in the EC specific attenuation and absorption cross-section efficiencies (σ_{ATN} and σ_{abs}) and are shown in Figure 6.

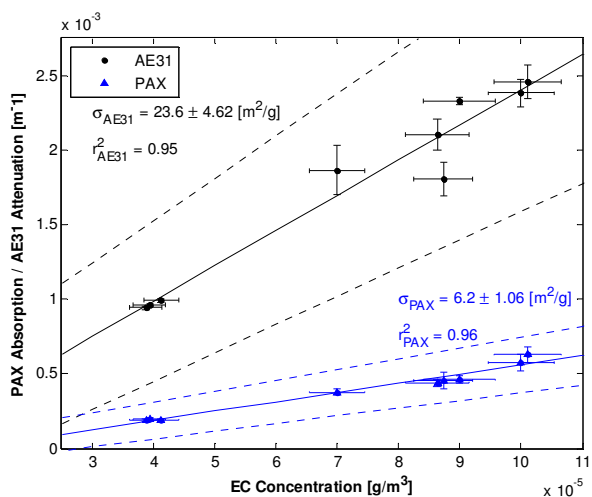


Figure 6: Aerosol Absorption and Attenuation vs NIOSH 5040 EC Concentration. Dashed lines represent the 95% confidence interval on the linear fit.

Dashed lines give the 95% confidence interval on the linear fit. The AE31 attenuation coefficient correlates well with EC concentration, yielding an R^2 value of 0.95. The PAX absorption coefficient also correlates well with EC concentration, resulting in an R^2 value of 0.96. The relative uncertainty for EC specific attenuation cross-section efficiency was 20%. This error can be attributed to lack of artifact correction to the AE31 attenuation signal and error in the EC measurement. The relative uncertainty for the EC specific absorption cross-section efficiency was 17%.

Traditionally, diesel PM is often thought to be composed mainly of carbonaceous particles which absorb light very efficiently, it is interesting to fit aerosol absorption to $PM_{2.5}$ mass. The result of this fit is presented in Figure 7.

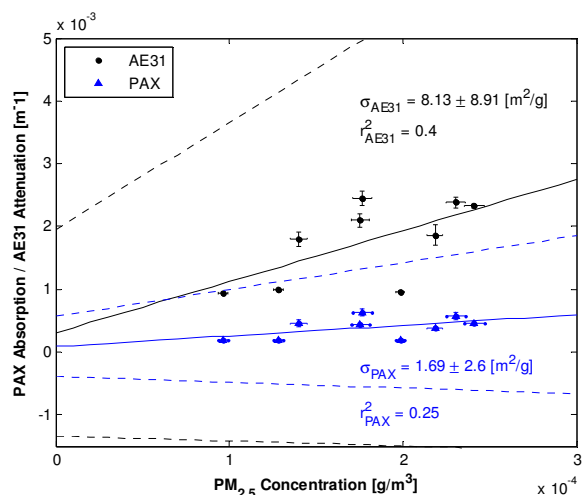


Figure 7: Aerosol Absorption and Attenuation vs. $PM_{2.5}$ Mass Concentration. Dashed lines represent the 95% confidence interval on the linear fit.

Dashed lines once again represent 95% confidence intervals on the linear fit. Unlike the EC fit, aerosol absorption and attenuation coefficients do not correlate well with $PM_{2.5}$ mass concentrations.

Summary/Conclusions

In this study, five different aerosol measurement techniques were compared to understand their suitability for determining aerosol black carbon mass concentration from modern diesel engines. Significant differences between measurement techniques were seen, but with proper understanding, each has its individual benefits and drawbacks. The following conclusions may be drawn from this study.

- The AE31 attenuation signal decayed over the sample period, indicating significant sampling artifacts, which need to be addressed when reporting BC concentrations with an AE31.
- The PAX and SMPS did not suffer from filter associated artifacts over the sample period due to their in-situ measurement techniques.
- For all engine modes tested, the DOC out PSDs were not geometrically different enough to affect aerosol absorption properties.
- The AE31 attenuation coefficient at 880 nm correlates well with NIOSH 5040 EC concentrations ($R^2 = 0.95$) resulting in a σ_{ATN} of $23.6 \pm 4.62 \text{ m}^2\text{g}^{-1}$. The measured σ_{ATN} is 30% higher than the manufacturer published σ_{ATN} .
- The PAX absorption coefficient at 870 nm correlates well with NIOSH 5040 EC concentrations ($R^2 = 0.96$) resulting in a σ_{ABS} of $6.20 \pm 1.06 \text{ m}^2\text{g}^{-1}$. The measured σ_{ABS} is 24% higher than the manufacturer published σ_{ABS} .

- These results indicate a difference in optical properties of the sampled aerosols as compared to the aerosols used to develop these instruments. A number of changes in diesel emissions control technology and sampling conditions (aged vs. fresh aerosol) could explain the differences in σ_{ATN} and σ_{ABS} .
- Both the AE31 attenuation and PAX absorption coefficients (b_{atn} and b_{abs}) do not correlate with $PM_{2.5}$ mass concentration.
- For measuring real time single wavelength aerosol absorption and scattering, the DMT PAX performed well with very dry and dilute exhaust sample.
- The AE31 allows for multiple wavelength aerosol absorption measurements in quasi-real time. Multiple wavelength attenuation permits researchers to investigate BrC emissions as well as BC. The AE31 suffers from filter artifacts, as expected, but are easily corrected with well-established methods. However, the AE31 has been discontinued and the new version has a built-in filter loading correction, the linear correction methodology has not been evaluated for use with diesel source emissions.

References

1. Kittleson, D.B., "Engines and nanoparticles: A review," *Journal of Aerosol Science* 29(5-6):575-588, 1998, doi:[10.1016/S0021-8502\(97\)10037-4](https://doi.org/10.1016/S0021-8502(97)10037-4).
2. U.S. Environmental Protection Agency (EPA), "Health assessment document for diesel engine exhaust," 2002, EPA/600/8-90/057F. Available from: <http://www.epa.gov/ncea>.
3. Pope, C.A., III, Thun, M.J., Namboodiri, M.M., Dockery, D.W., et al., "Particulate air pollution as a predictor of mortality in a prospective study of U.S. adults," *Am. J. Respir. Crit. Care Med.* 151(3 Pt 1):669-74, 1995.
4. Bond, T.C., and Bergstrom, R.W., "Light Absorption by Carbonaceous Particles: An Investigative Review," *Aerosol Science and Technology* 40(1):27-67, 2006, doi:[10.1080/02786820500421521](https://doi.org/10.1080/02786820500421521).
5. Maricq, M. M., "Chemical characterization of particulate emissions from diesel engines: A review." *Journal of Aerosol Science*. 38(11):1079-1118. 2007, doi:[10.1016/j.jaerosci.2007.08.001](https://doi.org/10.1016/j.jaerosci.2007.08.001)
6. Shindell, D., Kuylensstierna, J.C.I., Vignati, E., Dingenen, R., et al., "Simultaneously Mitigating Near-Term Climate Change and Improving Human Health and Food Security," *Science* 335(13):183-189, 2012, doi:[10.1126/science.1210026](https://doi.org/10.1126/science.1210026).
7. U.S. Environmental Protection Agency (EPA), "Report to Congress on Black Carbon," 2012, Available from:
8. Bahadur, R., Feng, Y., Russell, L.M., and Ramanathan, V., "Impact of California's air pollution laws on black carbon and their implications for direct radiative forcing," *Atmospheric Environment* 45(5):1162-1167, 2011, doi:[10.1016/j.atmosenv.2010.10.054](https://doi.org/10.1016/j.atmosenv.2010.10.054).
9. Moosmüller, H., Chakrabarty, R.K., and Arnott, W.P., "Aerosol light absorption and its measurement: A review," *Journal of Quantitative Spectroscopy and Radiative Transfer* 110(11):844-878, 2009, doi:[10.1016/j.jqsrt.2009.02.035](https://doi.org/10.1016/j.jqsrt.2009.02.035).
10. Arnott, W.P., Zielinska, B., Rogers, C.F., Sagebiel, J., et al., "Evaluation of 1047-nm Photoacoustic Instruments and Photoelectric Aerosol Sensors in Source-Sampling of Black Carbon Aerosol and Particle-Bound PAHs from Gasoline and Diesel Powered Vehicles," *Environmental Science and Technology* 39(14):5398-5406, 2005, doi:[10.1021/es049595e](https://doi.org/10.1021/es049595e).
11. Ban-Weiss, G.A., Lunden, M.M., Kirchstetter, T.W., and Harley, R.A., "Measurements of Black Carbon and Particle Number Emission Factors from Individual Heavy-Duty Trucks," *Environmental Science and Technology* 43(5):1419-1424, 2009, doi:[10.1021/es8021039](https://doi.org/10.1021/es8021039).
12. Dallmann, T.R., Harley, R.A., and Kirchstetter, T.W., "Effects of Diesel Particle Filter Retrofits and Accelerated Fleet Turnover on Drayage Truck Emissions at the Port of Oakland," *Environmental Science and Technology* 45(24):10773-10779, 2011, doi:[10.1021/es202609q](https://doi.org/10.1021/es202609q).
13. Hansen, A.D.A., and Rosen, H., "Individual Measurements of the Emission Factor of Aerosol Black Carbon in Automobile Plumes," *Journal of the Air and Waste Management Association* 40(12):1654-1657, 1990, doi:[10.1080/10473289.1990.10466812](https://doi.org/10.1080/10473289.1990.10466812).
14. Weingartner, E., Saathoff, H., Schnaiter, M., Streit, N., et al., "Absorption of light by soot particles: determination of the absorption coefficient by means of aethalometers," *Journal of Aerosol Science* 34(10):1445-1463, 2003, doi:[10.1016/S0021-8502\(03\)00359-8](https://doi.org/10.1016/S0021-8502(03)00359-8).
15. Moosmüller, H., Arnott, W.P., Rogers, C.F., Bowen, J.L., et al., "Time-Resolved Characterization of Diesel Particulate emissions. 2. Instruments for Elemental and Organic Carbon Measurements," *Environmental Science and Technology* 35(10):1935-1942, 2001, doi:[10.1021/es0015242](https://doi.org/10.1021/es0015242).
16. Ng, I., Ma, H., Kittelson, D., and Miller, A., "Comparing Measurements of Carbon in Diesel Exhaust Aerosols Using the Aethalometer, NIOSH Method 5040, and SMPS," SAE Technical Paper 2007-01-0334, 2007, doi:[10.4271/2007-01-0334](https://doi.org/10.4271/2007-01-0334).
17. Liu, G.Z., Vasys, V.N., Dettmann, M.E., Schauer, J.J., et al., "Comparison of Strategies for the Measurement of Mass Emissions from Diesel Engines Emitting Ultra-Low Levels of Particulate Matter," *Aerosol Science and Technology* 43(11): 1142-1152, 2009, doi:[10.1080/02786820903219035](https://doi.org/10.1080/02786820903219035)
18. Bohren, C.F., and Huffman, D.R., "Absorption and scattering of light by small particles," John Wiley and Sons, New York, 1983.
19. Bond, T.C., Habib, G., and Bergstrom, R.W., "Limitations in the enhancement of visible light absorption due to mixing state," *J. Geophys. Res.*, 111, D20211, 2006, doi:[10.1029/2006JD007315](https://doi.org/10.1029/2006JD007315).
20. Mätzler, C., "MATLAB Functions for Mie Scattering and Absorption," Institut für Angewandte Physik, Research Report No. 2002-08, Bern, Switzerland, 2002.
21. Liu, G.Z., Swor, T.A., Schauer, J.J., Debilzen, J.J., et al., "A Source Dilution Sampling System for Characterization of Engine emissions under Transient or Steady-State Operation," *Aerosol Science and Technology* 42(4):270-280, 2008, doi:[10.1080/02786820801992907](https://doi.org/10.1080/02786820801992907).
22. Collaud Coen, M., Weingartner, E., Apituley, A., Geburnis, D., et al., "Minimizing light absorption measurement artifacts of the Aethalometer: evaluation of five correction algorithms," *Atmospheric Measurement Techniques* 2:1725-1770, 2009, doi:[10.5194/amtd-2-1725-2009](https://doi.org/10.5194/amtd-2-1725-2009).
23. Droplet Measurement Technologies (DMT), "Photoacoustic Extinctionmeter (PAX) Operator Manual", 2012, Available from: www.dropletmeasurement.com
24. Liu, Z., Verdegan, B., Badeau, K., and Sonsalla, T., "Measuring the Fractional Efficiency of Diesel Particulate

Filters,” SAE Technical Paper 2002-01-1007, 2002, doi: [10.4271/2002-01-1007](https://doi.org/10.4271/2002-01-1007).

25. Dutton, S.J., Schauer, J.J., Vedal, S., and Hannigan, M.P., “PM2.5 characterization for time series studies: Pointwise uncertainty estimation and bulk speciation methods applied in Denver,” *Atmospheric Environment* 43(5):1136-1146, 2009, doi:[10.1016/j.atmosenv.2008.10.003](https://doi.org/10.1016/j.atmosenv.2008.10.003).

Contact Information

Correspondence should be addressed to: Michael A. Robinson at Cummins Emission Solutions, 1801 US Highway 51, Stoughton, WI 53589; ja665@cummins.com

Acknowledgments

This publication was made possible in part by US EPA grant 83503901. Its contents are solely the responsibility of the grantee and do not necessarily represent the official views of the US EPA. Further, US EPA does not endorse the purchase of any commercial products or services mentioned in the publication.

The authors would like to acknowledge Tony Hansen of Magee Scientific for valuable conversation and instrument availability. The authors would also like to acknowledge Bruce Ganrud of Droplet Measurement Technologies for instrument availability and testing support. The authors would like to acknowledge Paul Van Rooy of University of Wisconsin –Madison, Environmental Chemistry and Technology Department for help with setup and test execution. The authors also acknowledge Niklas Schmidt, Chris Cremeens, Nathan Ottinger, Nick Molzahn, Dustin Esteltine, Brad Nolley, and Jason Cassidy of Cummins Emission Solutions for their assistance with parts procurement, sampling, and testing support, as well as Shawn Hricko of Cummins Engine Business Unit for engine calibration support.

Definitions/Abbreviations

BC	Black Carbon
BrC	Brown Carbon
<i>b</i>_{ATN}	Attenuation Coefficient
<i>b</i>_{ABS}	Absorption Coefficient
CFV-CVS	Critical Flow Venturi Constant Volume System
CPC	Condensation Particle Counter

DMA	Differential Mobility Analyzer
DOC	Diesel Oxidation Catalyst
DPF	Diesel Particulate Filter
EC	Elemental Carbon
EGR	Exhaust Gas Recirculation
EPA	Environmental Protection Agency
FTIR	Fourier transform infrared spectroscopy
GHG	Green House Gas
IR	Infrared
λ	Wavelength
OC	Organic Carbon
PAX	Photoacoustic Extinctionmeter
PM	Particulate Matter
PM_{2.5}	Particulate Matter < 2.5 μ m
PSD	Particle Size Distribution
PSL	Poly-Styrene Latex
RTC	Residence Time Chamber
SCR	Selective Catalytic Reduction
SDS	Source Dilution Sampler
SMPS	Scanning Mobility Particle Sizer
σ_{ATN}	Attenuation Cross-Section Efficiency
σ_{ABS}	Absorption Cross-Section Efficiency
UV	Ultraviolet